VOL. 162, NO. 4 THE AMERICAN NATURALIST OCTOBER 2003

The Effects of the Size and Shape of Landscape Features on the Formation of Traveling Waves in Cyclic Populations

J. A. Sherratt,[1,*] **X. Lambin,**[2] **and T. N. Sherratt**[3,†]

1. Department of Mathematics, Heriot-Watt University, Edinburgh EH14 4AS, United Kingdom;
2. Aberdeen Population Ecology Research Unit, Department of Zoology, University of Aberdeen, Tillydrone Avenue, Aberdeen AB24 2TZ, United Kingdom;
3. Department of Biological Sciences, University of Durham, South Road, Durham DH1 3LE, United Kingdom

Submitted July 25, 2002; Accepted March 13, 2003; Electronically published October 16, 2003

Online enhancements: appendixes, figure.

ABSTRACT: Recent field data indicate that in a number of cyclic populations, the cycles are organized spatially with the form of a periodic traveling wave. One way in which this type of wave is generated is when dispersing individuals encounter landscape features that impede movement in certain directions. In this article, we investigate the dependence of such periodic waves on ecological parameters and on the form of the landscape feature. Using a standard predator-prey model as a prototype for a cyclic population, we calculate the speed and amplitude of waves generated by a large landscape feature. This enables us to determine parameters for which the waves are stable; in other cases, they evolve into irregular oscillations. We then undertake for the first time a detailed study of the effects of the size and shape of a landscape feature on the waves that it generates. We show that size rather than shape is the key wave-forming property, with smaller obstacles generating waves with longer wavelength and waves from larger landscape features dominating those from smaller ones. Our results suggest that periodic traveling waves may be much more common than has previously been assumed in real ecological systems, and they enable quantitative predictions on the properties of these waves for particular cases.

Keywords: traveling waves, population cycles, mathematical modeling.

It is well known that many natural populations are cyclic. The possibility of a spatial component to these oscillations was recognized over half a century ago in the case of Canadian lynx (*Lynx canadensis*; Elton and Nicholson 1942; see also Smith and Davis 1981), but detailed spatiotemporal studies have been attempted only recently. In several cases, this has revealed that the oscillations are organized into periodic traveling waves. This phenomenon has been studied in particular detail for field voles (*Microtus agrestis*) in the Kielder forest on the Scotland-England border (Lambin et al. 1998; MacKinnon et al. 2001) and red grouse (*Lagopus lagopus scoticus*) on Kerloch Moor in northeast Scotland (Moss et al. 2000). In both cases, recently developed statistical methods (Bjørnstad et al. 1999) have been applied to spatiotemporal data sets, revealing patterns consistent with periodic waves moving at a speed of 15–20 km/yr for field voles and 2–3 km/yr for red grouse. Other recent studies show periodic traveling waves in a range of ecological and epidemiological systems (Ranta and Kaitala 1997; Bjørnstad and Bascompte 2001; Grenfell et al. 2001).

The above observations raise the important issue of what it is that causes the periodic waves. In a previous article (Sherratt et al. 2002), we argued that such waves may be caused by landscape features that impede dispersal in certain directions. In the case of the field vole study, this would be Kielder water, a large reservoir in the center of the forest, and for the red grouse study, it would be the farmland and woodland adjacent to the study site. Despite their universality, landscape-mediated heterogeneities are rarely considered in spatiotemporal models, but it is becoming increasingly clear that they can have important effects on ecological dynamics (e.g., Wiegand et al. 1999).

In this article, we generate quantitative predictions on the ecological parameters required for landscape-generated periodic waves, on the way in which obstacle size and shape affect the period and amplitude of the wave, and on the way in which waves from different landscape features will interact. Although we focus on cyclic predator-prey systems, the methods that we describe could be applied in the same way to populations that cycle for other reasons,

---

[*] E-mail: jas@ma.hw.ac.uk.

[†] Present address: Department of Biology, Carleton University, Ottawa, Ontario KIS 5B6, Canada.

Am. Nat. 2003. Vol. 162, pp. 503–513.

such as the interaction between a pathogen and its host. We suggest that the generation of periodic waves by landscape features is a general property of cyclic populations rather than applying specifically to predator-prey systems, and we discuss this in more detail later in the article.

We begin by introducing the predator-prey model and summarizing the results from numerical solutions ("Simulation of Periodic Wave Generation"). We then describe the calculation of periodic wave stability ("Predicting Periodic Wave Stability") and discuss the effects of varying the size and shape of the landscape feature ("Periodic Waves in Two Dimensions").

Simulation of Periodic Wave Generation

In this article we consider only mathematical models of reaction-diffusion form, although periodic wave generation by landscape features is also predicted by coupled map lattice models (Sherratt et al. 2002). Our model equations are a standard predator-prey system:

$$\text{predators} \quad \frac{\partial p}{\partial T} = \overbrace{\nabla^2_{\underline{X}} p}^{\text{dispersal}} + \overbrace{\frac{ACph}{B(1 + Ch)}}^{\text{benefit from predation}} - \overbrace{\frac{p}{AB}}^{\text{death}} \tag{1a}$$

$$\text{prey} \quad \frac{\partial h}{\partial T} = \underbrace{\delta \nabla^2_{\underline{X}} h}_{\text{dispersal}} + \underbrace{h(1 - h)}_{\text{intrinsic birth and death}} - \underbrace{\frac{Cph}{(1 + Ch)}}_{\text{predation}}. \tag{1b}$$

These equations have been nondimensionalized (details in app. A), and $p(\underline{X},T)$ and $h(\underline{X},T)$ are predator and prey densities, respectively, functions of time T and space $\underline{X}$. We consider behavior in one space dimension initially and then extend to two dimensions ("Periodic Waves in Two Dimensions"). The dimensionless parameters A and B have simple ecological interpretations. The parameter A is the ratio of predator birth and death rates, and parameter B is the ratio of prey and predator birth rates. The parameter C reflects the rate at which prey consumption per predator saturates as prey density increases. Straightforward mathematical analysis shows that this model is oscillatory when C is above the critical value $(A + 1)/(A - 1)$; note that $A > 1$ is required for prey and predators to coexist. Clearly the ecological interpretation of the parameter C is less straightforward than for A and B, and it is often most convenient to work with $\mu = C - (A + 1)/(A - 1)$. For fixed A and B, a larger value of μ corresponds to larger amplitude population cycles. The parameter δ is the ratio of the predator and prey diffusion coefficients.

We consider initially the solutions of equations (1) on a homogeneous one-dimensional domain; the solutions depend on the conditions that apply on the two boundaries. With no-flux conditions at both ends, randomly generated initial conditions rapidly evolve to spatially uniform population cycles. "No-flux" means simply that individuals cannot enter or leave through the boundary; this is often a suitable condition at the edge of a domain, but it will not be appropriate for many landscape features, including those which alter the rules governing dispersal. In particular, for a landscape feature that constitutes a region of very poor habitat or that individuals would attempt to cross but would always or almost always fail, the appropriate boundary condition is to fix population densities at 0. In an extensive program of numerical solutions (Sherratt et al. 2002), we found that such conditions result in periodic traveling waves moving across the domain (fig. 1*a*). The waves move away from the boundary that corresponds to the obstacle edge. Our results indicate that this same qualitative behavior always occurs, with one exception. For some parameter values, the wave is unstable: it is visible close to the boundary that corresponds to the obstacle edge, but then it breaks up into irregular spatiotemporal oscillations (fig. 1*b*). From a practical viewpoint, periodic waves would not be found in field data in such cases, and an important objective of this article is to predict conditions on parameter values for which an obstacle generates stable periodic waves.

Predicting Periodic Wave Stability

A systematic investigation of wave stability is not feasible from numerical simulations alone and requires mathematical analysis of periodic wave solutions. This is not possible for equations as complex as equations (1). However, we have been able to get good insight into the way in which wave stability depends on parameters by studying the special case of $\delta = 1$ and C just above the critical value $(A + 1)/(A - 1)$, or equivalently μ small. The restriction to $\delta = 1$ is definitely unrealistic for most terrestrial predator-prey interactions, for which one typically expects predators to disperse further than their prey. However, it is a mathematical necessity, and numerical solutions indicate that the dependence of the solution form on kinetic parameters is relatively insensitive to δ. The condition that μ is small means that the population cycles are of low amplitude: specifically, the ratio of maximum : minimum prey density is approximately $1 + [8(A - 1)\mu]^{1/2}$ when μ is small (app. B in the online edition of the *American Naturalist*). Most real systems have cycles of higher amplitude than this, but our calculation will give valuable insights into the way in which wave stability depends on ecological parameters.

In this special case, the standard mathematical technique of normal form analysis (e.g., Guckenheimer and Holmes 1983) can be used to calculate a systematic approximation

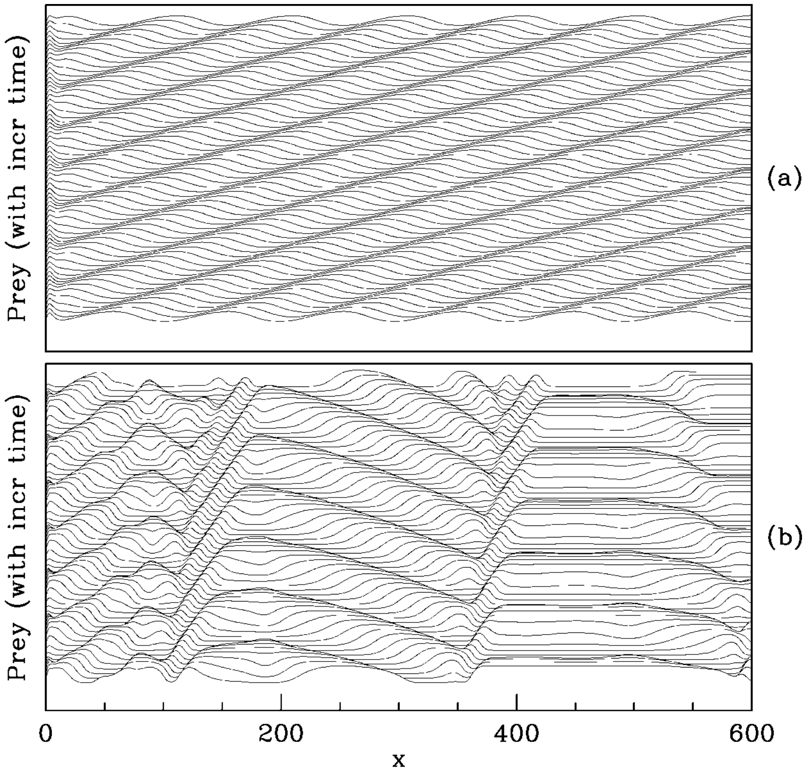

Figure 1: Generation of periodic waves by an obstacle edge in the predator-prey system (eqq. [1]). Zero population densities ($h = p = 0$) are imposed at $X = 0$ to simulate the edge of an obstacle, with zero flux conditions at the other boundary ($X = 600$). The boundary condition at $X = 0$ generates periodic traveling waves, which move away from the boundary. These waves can be either stable and persist (*a*) or unstable (*b*), in which case they develop into irregular spatiotemporal oscillations. The solutions for prey h are plotted at equally spaced times between $T = 3{,}850$ and $T = 4{,}000$ (time increasing up the page). The solutions for predators p are qualitatively similar. Initial conditions ($T = 0$) are given by generating random values of h and p between 0 and 1 at 60 equally spaced points in the domain and joining these by straight lines. The parameter values are (*a*) $A = 1.6$, $B = 1.2$, $C = 4.9$, $\delta = 2$; (*b*) $A = 1.8$, $B = 1.2$, $C = 6.0$, $\delta = 1$. The equations were solved numerically using a semi-implicit Crank-Nicolson method.

to the predator-prey model (1) of the following form, known as a "λ-ω" system:

$$\frac{\partial u}{\partial t} = \nabla^2_{\underline{x}} u + (1 - r^2)u - (\omega_0 - \omega_1 r^2)v, \qquad \text{(2a)}$$

$$\frac{\partial v}{\partial t} = \nabla^2_{\underline{x}} v + (\omega_0 - \omega_1 r^2)u + (1 - r^2)v, \qquad \text{(2b)}$$

where $r = (u^2 + v^2)^{1/2}$. The variables u and v are nonlinear combinations of p and h, with $u = v = 0$ corresponding to the coexistence equilibrium $h = h_s \equiv 1/[C(A-1)]$, $p = p_s \equiv Ah_s(1 - h_s)$. The parameters ω_0 and ω_1 depend on the ecological parameters as follows:

$$\omega_0 = \frac{2}{\mu}\left[\frac{A(A+1)}{(A-1)B}\right]^{1/2} + \left[\frac{A-1}{A(A+1)B}\right]^{1/2} \qquad \text{(3a)}$$

$$\omega_1 = \frac{4A^2B^2 + (A^2-1)(A^2+5)AB + (A^2-1)^2}{6A^{5/2}(A^2-1)^{1/2}B^{3/2}}. \qquad \text{(3b)}$$

The derivation of equations (3) is a standard "reduction to normal form" calculation, which we outline in appendix B. It involves a large amount of algebra that is best done computationally; we have used the package MAPLE, and the worksheet is available at the web site http://www.ma.hw.ac.uk/~jas/supplements/lovoles. One simple implication of equations (3) is that ω_0 and ω_1 have the same sign; this will be important later in the article.

The equations (2) are much more amenable to mathematical analysis than equations (1). In particular, Sherratt (2003) has calculated the periodic wave solution generated by obstacles in a system of the form (2), in one space dimension. This calculation uses a different condition than in the predator-prey simulations at the obstacle edge, but in appendix C in the online edition of the *American Naturalist* we show that the solution form applies despite this difference. This mathematical work, together with standard results on periodic wave stability in λ-ω equations

(Kopell and Howard 1973), implies that the condition for periodic wave stability is $|\omega_1| < 1.110468\ldots$. Using equation (3b), this gives a condition on A and B, which is algebraically complex and is best illustrated graphically, as in figure 2. Stable periodic waves occur at moderate ratios of predator birth : death rate and when the ratio of prey : predator birth rate is reasonably large. Wave direction can also be predicted using the approximate system (2). The results of Sherratt (2003) show that for system (2), the periodic waves generated by an obstacle can move either toward or away from the obstacle edge, depending on the values of ω_0 and ω_1. When $|\omega_0|$ is large, as in our application, the direction depends simply on whether ω_0 and ω_1 have the same or opposite signs; formulas (3) imply that the former case applies in our application, in which case the waves will always move away from the obstacle edge, as illustrated in figure 1*a*.

The stability condition shown in figure 2 applies only when C is just above the critical value $(A+1)/(A-1)$. However, the calculations in appendix C also enable prediction of how stability changes as C (or equivalently μ) increase. Figure 3 illustrates the results of this study, in which wave amplitude is plotted against μ for fixed A and B. The key implication of figure 3 is that although periodic waves are unstable when $\mu = 0$ for this A and B, the predicted wave amplitude increases with μ, with the wave becoming stable at $\mu \approx 0.3$.

The values of A and B used in figure 3 ($A = 1.8$, $B = 1.2$) are derived from crude estimates of dimensional parameters for the predation of field voles (*Microtus agrestis*) by weasels (*Mustela nivalis*); the basis for these parameter values is described elsewhere (Sherratt 2001; Sherratt et al. 2002). One of the best-studied examples of periodic traveling waves in a real ecological population is for field voles in Kielder forest (northern United Kingdom), where predation by weasels is one of a number of possible explanations for the cyclic dynamics of the voles (Turchin and Hanski 1997; Lambin et al. 2000; Korpimäki et al. 2002). Moreover, in the center of Kielder forest is a very large reservoir (~1,000 ha), which is a natural candidate as a landscape feature that might generate periodic waves. Precise formulation of boundary conditions at the reser-

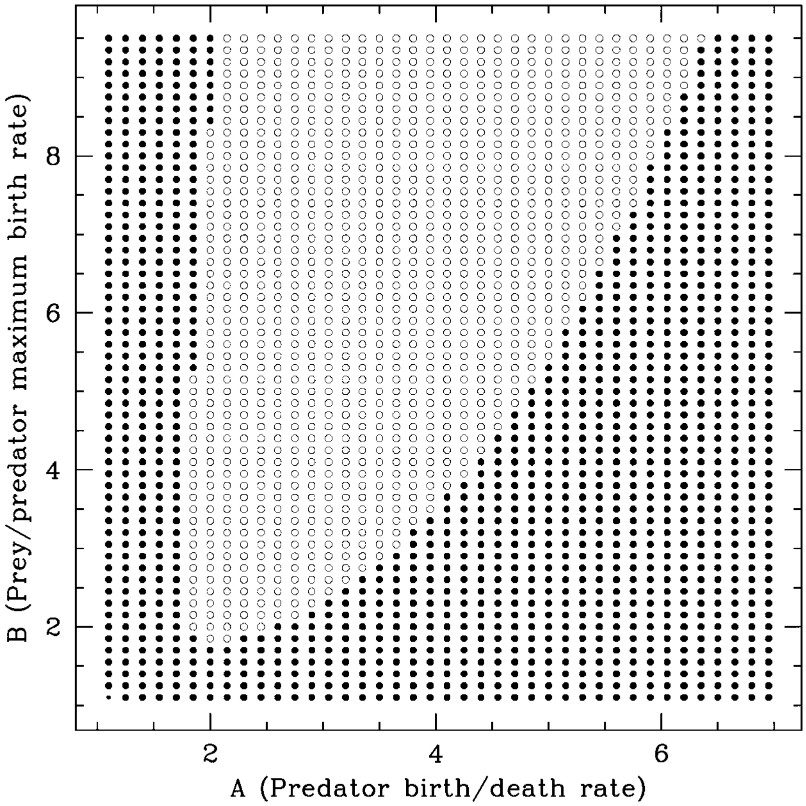

Figure 2: Condition on the parameters A and B for the periodic waves generated by an obstacle edge to be stable (*unfilled circles*) when the third parameter C is just above the critical value $(A+1)/(A-1)$ for cyclic behavior. In unstable cases (*filled circles*), waves will be generated but will gradually destabilize to give irregular spatiotemporal oscillations.

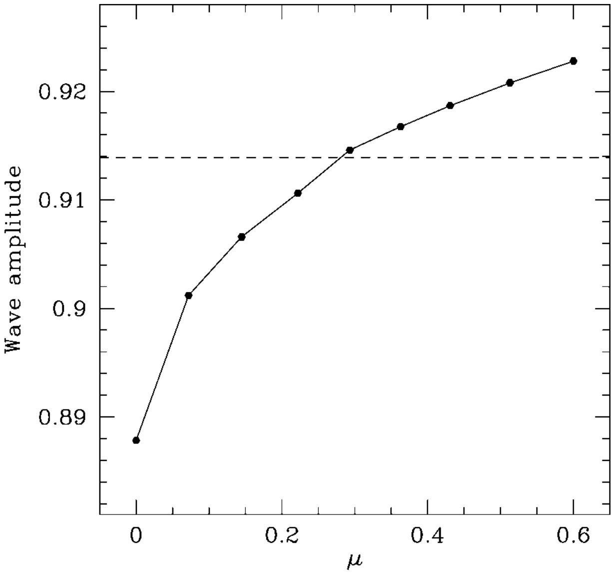

Figure 3: Predicted variation in periodic wave amplitude with the parameter $\mu = C - (A + 1)/(A - 1)$. The calculations used for this figure and the interpretation of the numerical values of wave amplitude are discussed in appendix B. The dashed line is the critical amplitude for stability: there is thus a transition from unstable to stable waves as μ increases. In this figure, $A = 1.8$ and $B = 1.2$, which are based on crude estimates for the weasel–field vole interaction. The results in this figure are only approximate for two reasons: first, due to high-order terms in μ being neglected, and second, because of the approximate nature of our calculation of r_{bdy}, which is explained at the end of appendix B.

voir edge is not possible because the details of vole behavior near the reservoir are not known. However, the vole density in the reservoir is certainly 0, so that setting vole density to 0 at the reservoir edge is certainly a plausible boundary condition.

An important question is therefore whether the parameter values for this interaction imply stable periodic wave generation by obstacles. Figure 3 implies that this depends on the third ecological parameter C (or equivalently μ). Our estimate of this parameter is $C = 4.9$, based on the amplitude of the field vole population cycle (Sherratt 2001; Sherratt et al. 2002). This corresponds to $\mu = 1.4$, which is clearly above the threshold for stability shown in figure 3. Our calculations do not really apply to such a large value of μ because they assume μ to be small, but they strongly suggest that the field vole–weasel interaction is within the parameter region giving stable periodic waves. The solution of the predator-prey equations in figure 1*a* is for the field vole–weasel parameters and demonstrates these stable waves.

Periodic Waves in Two Dimensions

Real terrestrial predator-prey interactions occur in two spatial dimensions. The analysis described above only applies in one dimension and cannot easily be extended to higher dimensions, but numerical solutions indicate that the key aspects of the results apply equally in two dimensions. Figure 4 illustrates the periodic waves generated by a central obstacle with population densities set to 0 at its edge; the shading corresponds to prey density, but the predator profile is very similar except for a phase difference. The waves have "target pattern" form and will approach a one-dimensional periodic wave as they move further away from the obstacle. The movement of the periodic waves can be seen in a movie clip corre sponding to this figure, which is available at http://www.ma.hw.ac.uk/˜jas/supplements/lovoles/.

An important new question arises in two space dimensions that has no equivalent in one dimension: how does obstacle size and shape affect the periodic waves? From an ecological viewpoint, this is a vital question relating to the type of landscape features that will tend to cause observable periodic waves in practice. Numerical investigation is hampered by the time-consuming nature of two-dimension simulations. Therefore, we approached the problem by considering the waves generated by circular obstacles of different sizes. The waves will then also be circular so that the problem is effectively one-dimensional, and an extensive program of numerical solutions is possible. As a measure of wave selection in these solutions, we calculated the spatial wavelength. This will, of course, vary with distance from the obstacle as the curvature of the wave changes, and we calculated the wavelength far from the obstacle. Here, the curvature of the waves is effectively negligible, but nevertheless their wavelength is significantly affected by the radius of the obstacle, as illustrated in figure 5. In this figure, we again use parameter values corresponding to the vole-weasel interaction, and we have converted dimensionless lengths into kilometers using these estimates. These results show that sufficiently large circular obstacles generate waves of the same wavelength as those found in the one-dimensional simulations discussed above. However, as the obstacle radius is decreased, the selected wave gradually changes, with wavelength increasing. As the obstacle becomes even smaller, the wavelength becomes even longer, and in the limiting case of a "point obstacle" (zero radius), the solution has the form of just homogeneous oscillations, which are equivalent to periodic waves of infinite wavelength.

When obstacles are not circular, numerical solutions in two dimensions are required, making a comprehensive study difficult. However, the simulations that we have done suggest that the main determinant of the periodic wave is

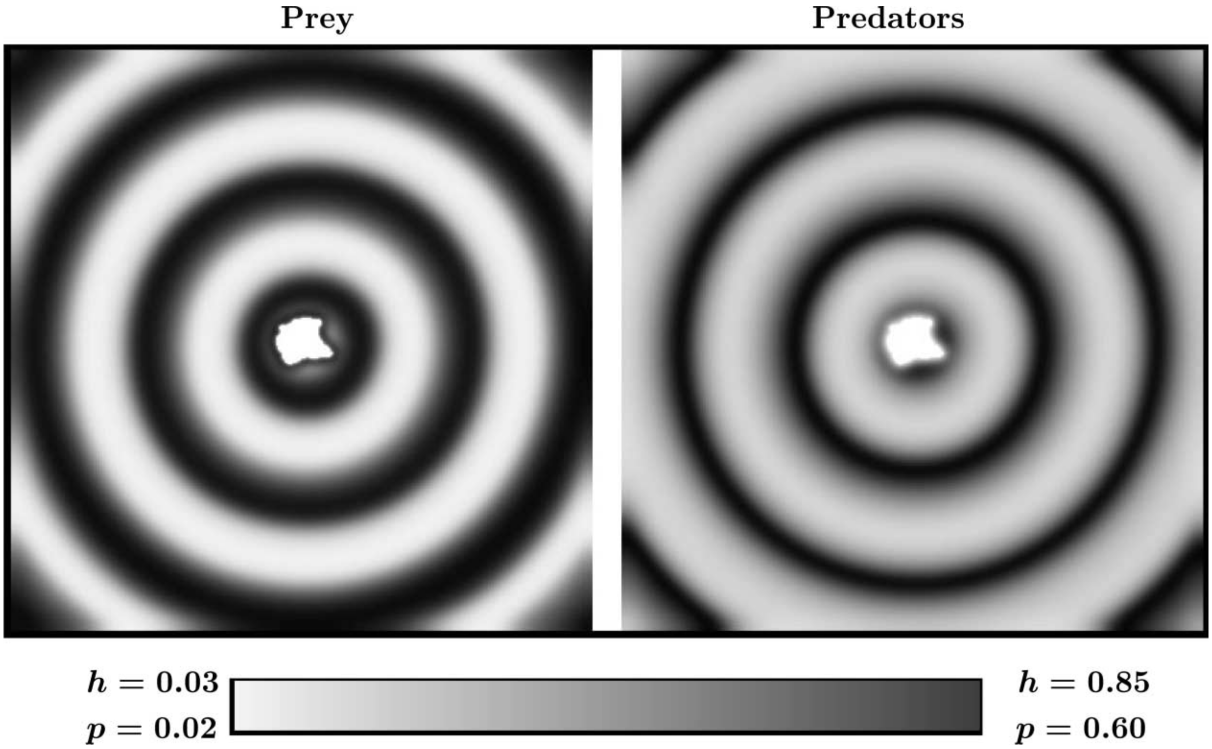

Figure 4: Periodic traveling waves in two space dimensions, generated by a central obstacle, for the predator-prey model (1). We plot prey and predator density as a function of space at one time point; the periodic waves move away from the obstacle. The boundary conditions are zero population densities at the edge of the obstacle and zero flux at the edge of the domain. The parameter values are $A = 1.8$, $B = 1.2$, $C = 4.9$, and $\delta = 2$, and the domain is a square of side length 400; the solution is plotted after 900 time units, with initial conditions generated randomly. These parameter values are based on crude estimates for the field vole–weasel interaction (Sherratt 2001; Sherratt et al. 2002), and the dimensionless domain length would then be ∼100 km. The equations were solved numerically using an alternating direction implicit implementation of the Crank-Nicolson scheme. A movie clip corresponding to this figure is available at http://www.ma.hw.ac.uk/˜jas/supplements/lovoles/.

the largest dimension of the obstacle generating it. This is illustrated in figure 6, where we plot the wavelength of periodic waves generated by rectangular obstacles of aspect ratio (length : width) 3 as a function of the longest side length. The wavelength of waves generated by circular obstacles for the same parameters is also shown for comparison. This shows that obstacle shape does not have a significant effect on periodic wave solutions in comparison to the effect of obstacle size.

In a real ecological domain, there are probably a considerable number of small obstacles as well as possibly one or more that are large. The different sizes of obstacle will then generate different periodic waves, and it is clearly important to consider what will emerge from the interaction of these waves. Insight into this comes from returning to the λ-ω system (2) discussed in "Predicting Periodic Wave Stability." Numerical solutions of these equations show that when different periodic waves are generated in different regions of space, a moving transition develops with one periodic wave invading the other (fig. 7*a*).

Careful numerical study shows that this transition moves with constant shape and speed in the wave amplitude r and phase gradient θ_x (fig. 7*b*), where r and θ are polar coordinates in the u–v plane. Substituting solutions of the form $r = R(z)$, $\theta_x = \Psi(z)$, and $z = x - at$ into equations (2) gives

$$R'' + aR' + R(1 - R^2 - \Psi^2) = 0, \tag{4a}$$

$$\Psi' + \frac{2\Psi R'}{R} + a\Psi + \omega_0 - \omega_1 R^2 = k, \tag{4b}$$

where k is a constant of integration. We denote by R_l, Ψ_l and R_r, Ψ_r the (constant) amplitude and phase gradient of the periodic wave to the left and right, respectively, of the transition. Substituting these into equation (4b) and subtracting implies

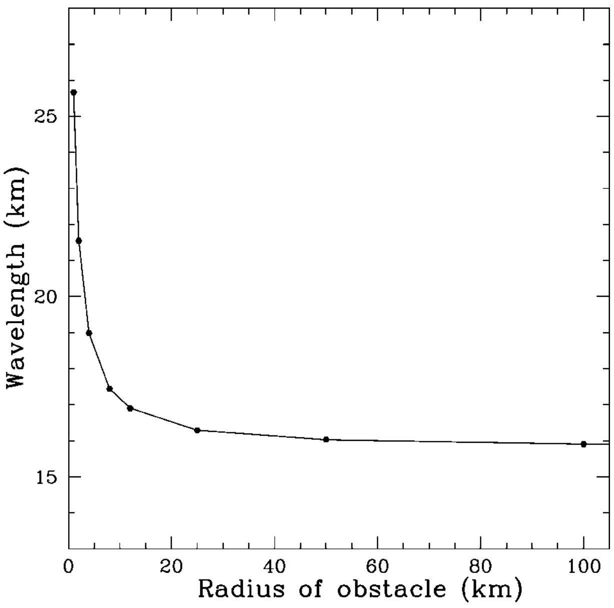

Figure 5: Illustration of the dependence of wavelength on the radius of the circular obstacle generating the periodic wave. We solve the predator-prey equations (1) on a domain that is circularly symmetric with the obstacle at the center. The wavelength is measured away from either the obstacle or domain edge after 3,000 dimensionless time units, by which time the long-term solution structure has developed. The dimensionless parameter values are as in figure 4, and the dimensionless lengths have been converted to kilometers using the parameter estimates for the field vole–weasel interaction (Sherratt 2001; Sherratt et al. 2002).

$$a = \frac{\omega_1(R_r^2 - R_l^2)}{\Psi_r - \Psi_l}.$$

We have shown that in predator-prey systems, periodic waves move away from the obstacle generating them. If the periodic waves on either side of the transition are generated by obstacles far to the left and right, and assuming $\omega_0 \gg \omega_1 > 0$ as implied by equations (3), this corresponds to $\Psi_r > 0$ and $\Psi_l < 0$. Therefore, a is positive if $R_r > R_l$ and negative otherwise, so that the periodic wave of smaller amplitude, and thus of smaller wavelength, invades that of larger amplitude (and wavelength). This is illustrated in figure 7.

When combined with the results illustrated in figure 5, this calculation implies the following simple result: the periodic waves generated by larger obstacles will outcompete those generated by smaller obstacles. For the predator-prey model (1), this is illustrated in figure 8. Here we have placed different sized obstacles in opposite corners of a square domain. Both generate periodic waves, and the longer wavelength of those generated by the smaller obstacle is very clear. In due course, the two periodic waves meet and begin to interact, and the wave generated by the smaller obstacle recedes. A movie clip corresponding to figure 8 is available at http://www.ma.hw.ac.uk/~jas/supplements/lovoles/.

Discussion

Periodic traveling wave solutions of oscillatory systems have been studied mathematically for about 30 yr, and applications in physiology and chemistry are well established (Williams et al. 1990; Winfree 2001). However, it is only in the last few years that their importance in ecology has been appreciated. Analysis of spatiotemporal data on cyclic populations has shown periodic traveling waves in a number of natural populations, with some of the most detailed studies covering field voles (Lambin et al. 1998; MacKinnon et al. 2001) and red grouse (Moss et al. 2000), both in the northern United Kingdom. Determination of the mechanism causing these waves is a major challenge for theoreticians. We have previously proposed landscape features as a possible mechanism for the generation of periodic waves (Sherratt et al. 2002). Here, we have significantly developed this theory, focussing on quantitative prediction of the parameter regimes in which stable periodic waves are expected and on the properties of these waves in two dimensions.

We have restricted attention to the specific case of cyclic predator-prey systems. However, we believe that the generation of periodic waves by landscape features will also apply to ecological systems that oscillate for other reasons, such as parasitism. This belief is based on the work we have described for λ-ω equations. Because these equations are the normal form for any simple oscillatory system, behavior seen in them will occur quite generally. The specific calculations leading to equations (3) and figure 2 are, of course, only applicable to the predator-prey model (1), but corresponding calculations can be done for other systems using the methods outlined in appendix B.

A factor that is missing from our model but that will be present in any real ecological system is environmental stochasticity. We have not attempted a systematic study of the wide range of possible stochastic effects, but as a particular example we considered the effects of random noise in the carrying capacity of the prey population. As one would expect, such noise has little effect when its amplitude is low, but at a relatively high amplitude (e.g., ±20% of the mean level), an effect is clearly visible (not illustrated for brevity). Surprisingly, a key additional factor was the spatial frequency over which the carrying capacity fluctuated. High frequency noise causes relatively minor modulations of the periodic wave pattern produced by obstacles, such as ruffling of wave fronts. But lower frequency fluctuations in carrying capacity can dominate the wave pattern, with periodic waves forming around extreme val-

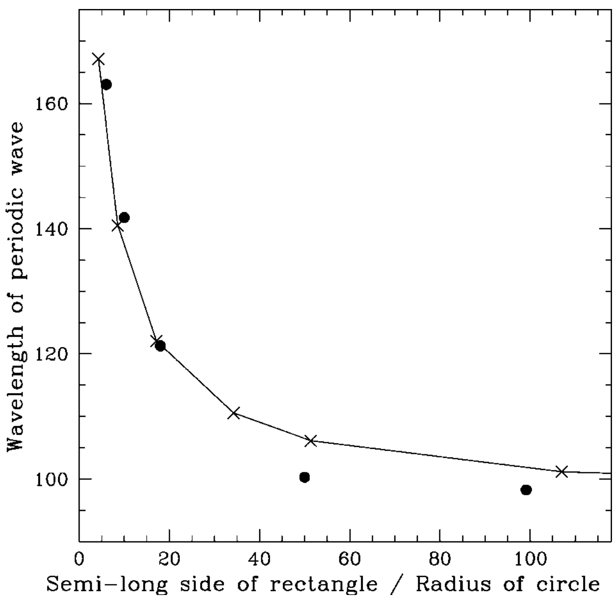

Figure 6: Comparison of the wavelengths of periodic waves generated by rectangular (*filled circles*) and circular (*crosses*) obstacles of different sizes. In each case the rectangular obstacles have an aspect ratio of 3 : 1, and half of the longer side length is plotted on the horizontal axis. The close correspondence between the results for the two obstacle shapes shows that the key factor controlling wavelength is the longest overall dimension of the obstacle, with obstacle shape playing a relatively minor role. The dimensionless parameter values are $A = 1.6$, $B = 1.2$, $C = 4.9$, and $\delta = 2$. In contrast to figure 5, these parameters do not correspond to a particular ecological system, and thus the distances plotted are dimensionless. Readers considering reproducing these results should be warned that the computations for the rectangular obstacles are very time consuming. We solved on a spatial domain that is square with dimensionless side length 400 and with the obstacle in one corner. This relatively large domain is required for there to be several full wavelengths away from both the obstacle and domain edges. We solved for 4,000 time units, which is sufficient for the long-term solution to develop. Each simulation takes about 30 h on our alpha processor.

ues of the carrying capacity rather than around the obstacle. This illustrates the way in which the wave-generation capacity of obstacles must be considered in parallel with other aspects of the local environment.

In spatially discrete populations, periodic traveling waves can arise spontaneously from small random fluctuations in density (Kaitala and Ranta 1998; Sherratt et al. 2000). However, this behavior depends intrinsically on the discreteness of the simulation and does not apply to continuous systems, where a specific mechanism of periodic wave generation is required. In applications to chemistry and physiology, a variety of such mechanisms has been studied (e.g., Hagan 1981; Kopell et al. 1991). Within ecology, invasion has been the most widely studied mechanism; for example, the invasion of a prey population by predators can leave behind periodic waves (Sherratt et al. 1995, 1997; Petrovskii and Malchow 2000, 2001). As in the results we have described, such an invasion can in some cases generate a periodic wave that is unstable and that develops into irregular spatiotemporal oscillations. Sherratt (2001) previously derived conditions on the parameters in the model (1) for stability of the periodic waves generated by invasion, and it is instructive to compare the results of that study with those derived in the present article. Specifically, for wave generation by invasion, there is a direct analog of the plot in figure 2, which shows the region of *A*-*B* parameter space giving stable waves when *C* is just large enough to give population cycles; the analogous figure is presented in Sherratt (2001). The two figures have the same qualitative form, although the param-

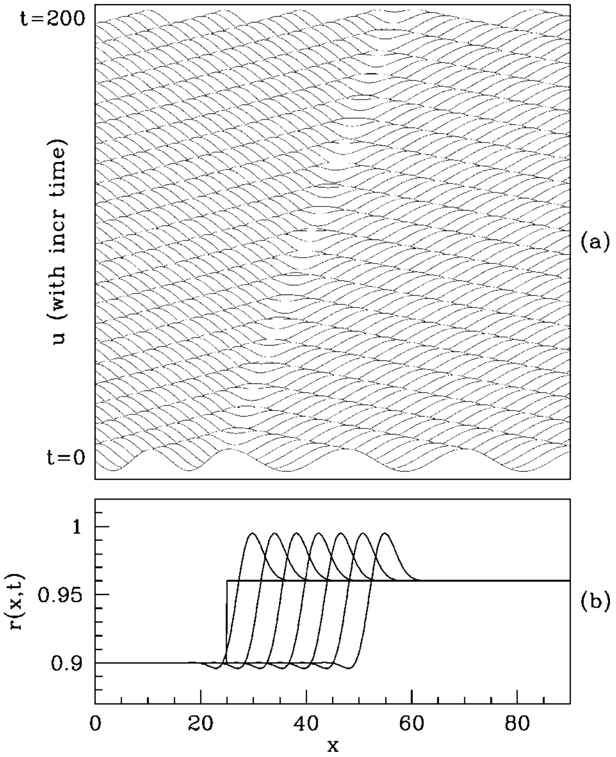

Figure 7: Illustration of the moving transition between periodic waves of different wavelengths for the λ-ω system (2). In *a* we show a space-time plot for $u(x, t)$, and in *b* we plot the solution amplitude $r(x, t)$ as a function of space at equally spaced times (time interval 26.7). As initial conditions, we impose a periodic wave of amplitude 0.9 in the region $x < 25$ and a wave of amplitude 0.96 on the remainder of the domain. The smaller amplitude wave invades the larger amplitude wave for reasons discussed in the main text. In this simulation, the waves are not generated by obstacles. Rather, they are maintained artificially by the boundary conditions $u_x = +v(1 - R_l^2)^{1/2}$ and $v_x = -u(1 - R_l^2)^{1/2}$, with $R_l = 0.9$ on the left-hand boundary and $u_x = -v(1 - R_r^2)^{1/2}$ and $v_x = +u(1 - R_r^2)^{1/2}$ with $R_r = 0.96$ on the right-hand boundary. These conditions correspond to $r = R_l$, $\theta_x = +[\lambda(R_l)]^{1/2}$ and $r = R_r$, $\theta_x = -[\lambda(R_r)]^{1/2}$, respectively. The parameter values are $\omega_0 = 1.5$, $\omega_1 = 1$.

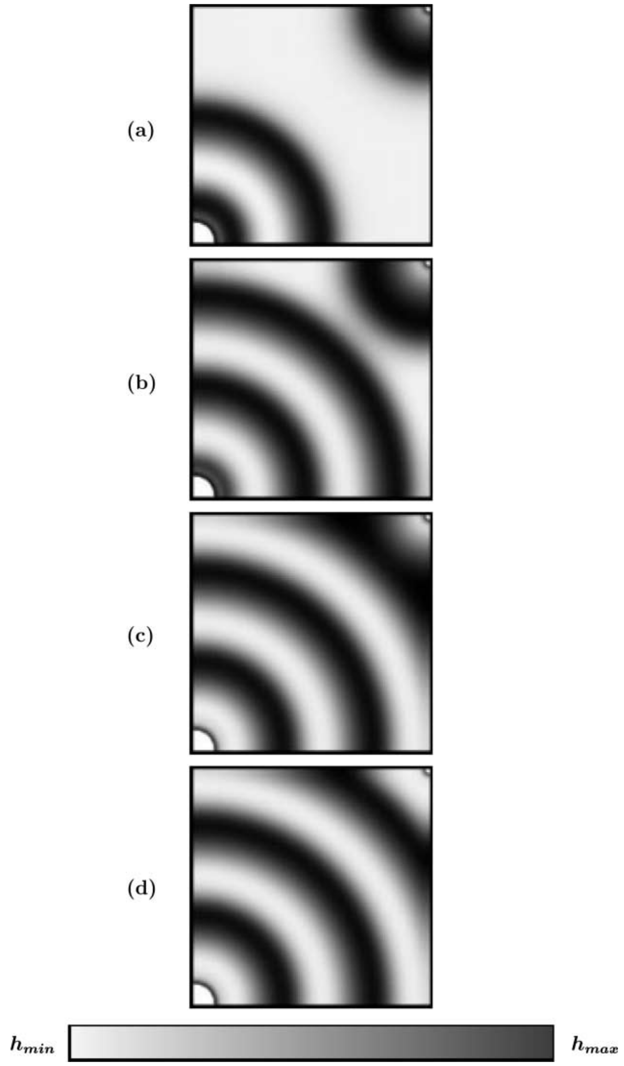

Figure 8: Illustration of the interaction between periodic waves generated by obstacles of different sizes for the predator-prey model (1). The model is solved with randomly generated initial population densities, which rapidly evolve toward homogeneous oscillations. The two obstacles, which are quarter circles of different radii in opposite corners of the domain, each generate periodic waves, which are clearly visible early in the solution (*a*). Note that the wavelength is significantly larger for the smaller obstacle. In due course the two sets of waves meet (*b*). The longer wavelength waves quickly begin to recede (*c*), so that at large times (*d*) the waves generated by the larger obstacle dominate. The parameter values are $A = 1.6$, $B = 1.2$, $C = 4.9$, and $\delta = 2$, and the spatial domain is a square of dimensionless length 300. The obstacles in the corners have radii 25 and 4. The solutions are plotted at times (*a*) 1,200, (*b*) 2,300, (*c*) 3,300, and (*d*) 7,300. The boundary conditions on the edge of the square domain are zero flux, with $h = p = 0$ on the obstacle edges. This figure is very computationally intensive, taking about a week to run on our alpha processor. A movie clip corresponding to this figure is available at http://www.ma.hw.ac.uk/˜jas/supplements/lovoles/.

eter region giving stable waves is slightly larger for wave generation by obstacles, compared to invasion. But the key difference lies in the effects of increasing C giving larger amplitude cycles; recall that C reflects the rate at which prey consumption per predator saturates as prey density increases. Increasing C has a relatively small effect on stability in the invasion case; mathematically, there is no change in stability to leading order in the small parameter μ. However, for wave generation by obstacles, increasing μ has a very significant stabilizing effect, as illustrated in figure 3. For this reason, we predict that the presence of landscape features is a much more widely applicable mechanism than predator invasion for the generation of stable periodic traveling waves in cyclic predator-prey systems. Moreover, the relationship we have derived between obstacle size and wavelength suggests that only large obstacles generate waves with a wavelength short enough to be easily detected, with many waves that arise from small obstacles going undetected.

Our work highlights the importance of understanding the way in which natural populations respond to the edges of landscape features. This has been best studied for butterflies (Dover and Fry 2001; Ries and Debinski 2001) and songbirds (Belisle and Clair 2002; Belisle and Desrochers 2002), revealing a strong tendency to avoid crossing habitat boundaries. For instance, Belisle and Desrochers (2002) found that forest birds attracted to a mobbing call preferred to travel under forest cover rather than using significantly shorter routes across open areas. For mammals, direct analysis of behavior at barrier edges is rare. Examples include the work of Rondinini and Doncaster (2002) demonstrating the tendency of hedgehogs (*Erinaceus europaeus L.*) to avoid crossing large (but not small) roads and the work of Bright (1998) showing that dormice (*Muscardinus avellanarius*) are averse to crossing even small gaps in hedgerows. In addition to this direct observational data, there is some genetic evidence that landscape features may reduce dispersal. For example, Piertney et al. (1998) found genetic differences between populations of red grouse (*Lagopus lagopus scoticus*) on either side of an area of unsuitable habitat, showing that this area acts as an effective barrier to movement. Similarly, Gerlach and Musolf (2000) used genetic data to demonstrate significant subdivision of bank vole (*Clethrionomys glareolus*) populations separated by a highway. We anticipate that, as further data emerge on responses to landscape features, theoretical modeling of the type we have presented will reveal further details of the implications that such data have for overall population dynamics.

Acknowledgments

J.A.S. was supported in part by an Advanced Research Fellowship from Engineering and Physical Sciences Research Council. X.L. was supported by a fellowship from the Leverhulme Trust and by a research grant from the Natural Environment Research Council (NERC). T.N.S. was supported in part by NERC and the Scottish Office under the Large-Scale Processes in Ecology and Hydrology Thematic Programme (GST/02/1218).

APPENDIX A

In this appendix, we discuss the nondimensionalization that gives the predator-prey model (1) used in the article. The dimensional equations we use are a standard predator-prey model:

$$\text{predators}\quad \frac{\partial p}{\partial T} = \overbrace{D_p\nabla^2 p}^{\text{dispersal}} + \overbrace{\frac{akph}{(1+kh)}}^{\text{benefit from predation}} - \overbrace{bp}^{\text{death}}, \tag{A1a}$$

$$\text{prey}\quad \frac{\partial h}{\partial T} = \underbrace{D_h\nabla^2 h}_{\text{dispersal}} + \underbrace{rh\left(\frac{1-h}{h_0}\right)}_{\text{intrinsic birth and death}} - \underbrace{\frac{ckph}{(1+kh)}}_{\text{predation}}. \tag{A1b}$$

Here *a*, *b*, *c*, *r*, *k* and h_0 are positive kinetic parameters, and D_p and D_h are dispersal coefficients. The prey consumption rate per predator has a maximal value *c* at very high prey densities; the constant *k* reflects how quickly the consumption rate decreases as prey density increases. Parameters *a* and *r* denote maximal per capita predator and prey birth rates; for predators, that is the birth rate when the prey density is very high, while for prey, it is the birth rate at very low prey density. The per capita predator death rate is denoted by *b*, and h_0 is the prey carrying capacity. We nondimensionalize equations (A1) using the rescalings

$$p^* = p\frac{c}{rh_0},\ h^* = \frac{h}{h_0},\ T^* = rT,\ \underline{X}^* = \underline{X}\sqrt{\frac{r}{D_\mathrm{h}}},$$

$$\delta^* = \frac{D_\mathrm{p}}{D_\mathrm{h}},\ A^* = \frac{a}{b},\ B^* = \frac{r}{a},\ C^* = kh_0, \tag{A2}$$

where the asterisks denote a dimensionless quantity. The interpretations of *A*, *B*, and *C*, as discussed in the main text, arise from these rescalings. Substituting equation (A2) into equations (A1) and dropping the asterisks give the dimensionless equations (1) in the main text.

Literature Cited

Belisle, M., and C. C. S. Clair. 2002. Cumulative effects of barriers on the movements of forest birds. Conservation Ecology 5:9 (online) http://www.consecol.org/vol5/iss2/art9.

Belisle, M., and A. Desrochers. 2002. Gap-crossing decisions by forest birds: an empirical basis for parameterizing spatially-explicit, individual-based models. Landscape Ecology 17:219–231.

Bjørnstad, O. N., and J. Bascompte. 2001. Synchrony and second-order spatial correlation in host-parasitoid systems. Journal of Animal Ecology 70:924–933.

Bjørnstad, O. N., R. A. Ims, and X. Lambin. 1999. Spatial population dynamics: analyzing patterns and processes of population synchrony. Trends in Ecology & Evolution 14:427–432.

Bright, P. W. 1998. Behaviour of specialist species in habitat corridors: arboreal dormice avoid corridor gaps. Animal Behaviour 56:1485–1490.

Dover, J. W., and G. L. A. Fry. 2001. Experimental simulation of some visual and physical components of a hedge and the effects on butterfly behaviour in an agricultural landscape. Entomologia Experimentalis et Applicata 100:221–233.

Elton, C., and M. Nicholson. 1942. The ten-year cycle in numbers of the lynx in Canada. Journal of Animal Ecology 11:215–244.

Gerlach, G., and K. Musolf. 2000. Fragmentation of landscape as a cause for genetic subdivision in bank voles. Conservation Biology 14:1066–1074.

Grenfell, B. T., O. N. Bjørnstad, and J. Kappey. 2001. Travelling waves and spatial hierarchies in measles epidemics. Nature 414:716–723.

Guckenheimer, J., and P. Holmes. 1983. Nonlinear oscillations, dynamical systems and bifurcations of vector fields. Springer, Berlin.

Hagan, P. S. 1981. Target patterns in reaction-diffusion systems. Advances in Applied Mathematics 2:400–416.

Kaitala, V., and E. Ranta. 1998. Travelling wave dynamics and self-organisation in a spatio-temporally structured population. Ecology Letters 1:186–192.

Knobloch, E. 1986 Normal form coefficients for the nonresonant double Hopf bifurcation. Physics Letters A 116: 365–369.

Kopell, N., and L. N. Howard. 1973. Plane wave solutions to reaction-diffusion equations. Studies in Applied Mathematics 52:291–328.

Kopell, N., G. B. Ermentrout, and T. L. Williams. 1991. On chains of oscillators forced at one end. SIAM Journal on Applied Mathematics 51:1397–1417.

Korpimäki, E., K. Norrdahl, T. Klemola, T. Pettersen, and N. C. Stenseth. 2002. Dynamic effects of predators on cyclic voles: field experimentation and model extrapolation. Proceedings of the Royal Society of London B, Biological Sciences 269:991–997.

Lambin, X., D. A. Elston, S. J. Petty, and J. L. MacKinnon. 1998. Spatial asynchrony and periodic travelling waves in cyclic populations of field voles. Proceedings of the Royal Society of London B, Biological Sciences 265: 1491–1496.

Lambin, X., S. J. Petty, and J. L. MacKinnon. 2000. Cyclic dynamics in field vole populations and generalist predation. Journal of Animal Ecology 69:106–118.

MacKinnon, J. L., X. Lambin, D. A. Elston, C. J. Thomas, T. N. Sherratt, and S. J. Petty. 2001. Scale invariant spatio-temporal patterns of field vole density. Journal of Animal Ecology 70:101–111.

Moss, R., D. A. Elston, and A. Watson. 2000. Spatial asynchrony and demographic travelling waves during red grouse population cycles. Ecology 81:981–989.

Petrovskii, S. V., and H. Malchow. 2000. Critical phenomena in plankton communities: KISS model revisited. Nonlinear Analysis: Real World Applications 1:37–51.

———. 2001. Wave of chaos: new mechanism of pattern formation in spatio-temporal population dynamics. Theoretical Population Biology 59:157–174.

Piertney, S. B., A. D. C. MacColl, P. J. Bacon, and J. F. Dallas. 1998. Local genetic structure in red grouse (*Lagopus lagopus scoticus*): evidence from microsatellite DNA markers. Molecular Ecology 7:1645–1654.

Ranta, E., and V. Kaitala. 1997. Travelling waves in vole population dynamics. Nature 390:456.

Ries, L., and D. M. Debinski. 2001. Butterfly responses to habitat edges in the highly fragmented prairies of central Iowa. Journal of Animal Ecology 70:840–852.

Rondinini, C., and C. P. Doncaster. 2002. Roads as barriers to movement for hedgehogs. Functional Ecology 16: 504–509.

Sherratt, J. A. 2001. Periodic travelling waves in cyclic predator-prey systems. Ecology Letters 4:30–37.

———. 2003. Periodic travelling wave selection by Dirichlet boundary conditions in oscillatory reaction-diffusion systems. SIAM Journal on Applied Mathematics 63:1520–1538.

Sherratt, J. A., M. A. Lewis, and A. C. Fowler. 1995. Ecological chaos in the wake of invasion. Proceedings of the National Academy of Sciences of the USA 92:2524–2528.

Sherratt, J. A., B. T. Eagan, and M. A. Lewis. 1997. Oscillations and chaos behind predator-prey invasion: mathematical artifact or ecological reality? Philosophical Transactions of the Royal Society of London B, Biological Sciences 352:21–38.

Sherratt, J. A., X. Lambin, C. J. Thomas, and T. N. Sherratt. 2002. Generation of periodic waves by landscape features in cyclic predator-prey systems. Proceedings of the Royal Society of London B, Biological Sciences 269:327–334.

Sherratt, T. N., X. Lambin, S. J. Petty, J. L. MacKinnon, C. F. Coles, and C. J. Thomas. 2000. Application of coupled oscillator models to understand extensive synchrony domains and travelling waves in populations of the field vole in Kielder Forest, UK. Journal of Applied Ecology 37(suppl. 1):148–158.

Smith, C. H., and J. M. Davis. 1981. A spatial analysis of wildlife's ten-year cycle. Journal of Biogeography 8:27–35.

Turchin, P., and I. Hanski. 1997. An empirically based model for latitudinal gradient in vole population dynamics. American Naturalist 149:842–874.

Wiegand, T., K. A. Moloney, J. Naves, and F. Knauer. 1999. Finding the missing link between landscape structure and population dynamics: a spatially explicit perspective. American Naturalist 154:605–627.

Williams, T. L., K. A. Sigvardt, N. Kopell, G. B. Ermentrout, and M. P. Remler. 1990. Forcing of coupled nonlinear oscillators: studies of intersegmental coordination in the lamprey locomotor central pattern generator. Journal of Neurophysiology 64:862–871.

Winfree, A. T. 2001. The geometry of biological time. Springer, New York.

Associate Editor: Rolf A. Ims